Soy genistein administered in soluble chitosan microcapsules maintains antioxidant activity and limits intestinal inflammation

Vanden Braber, Novotny Nuñez, L. Bohl, C. Porporatto, FN. Nazar, MA Montenegro, SG. Correa

PII: S0955-2863(18)30311-5
DOI: doi:10.1016/j.jnutbio.2018.08.009
Reference: JNB 8039

To appear in: *The Journal of Nutritional Biochemistry*

Received date: 3 April 2018
Revised date: 29 July 2018
Accepted date: 24 August 2018

Please cite this article as: Vanden Braber, Novotny Nuñez, L. Bohl, C. Porporatto, FN. Nazar, MA Montenegro, SG. Correa , Soy genistein administered in soluble chitosan microcapsules maintains antioxidant activity and limits intestinal inflammation. Jnb (2018), doi:10.1016/j.jnutbio.2018.08.009

Soy genistein administered in soluble chitosan microcapsules maintains antioxidant activity and limits intestinal inflammation

Vanden Braber NL, PhD[1], Novotny Nuñez I, PhD[2], Bohl L, PhD[1], Porporatto C, PhD[1], Nazar FN, PhD[3], Montenegro MA, PhD[1], Correa SG, PhD[2]*

[1]Centro de Investigaciones y Transferencia de Villa María (CITVM-CONICET), Universidad Nacional de Villa María, Villa María, Córdoba, Argentina.

[2]Centro de Investigación en Bioquímica Clínica e Inmunología (CIBICI-CONICET), Departamento de Bioquímica Clínica-Facultad de Ciencias Químicas, Universidad Nacional de Córdoba, Córdoba, Argentina.

[3]Instituto de Investigaciones Biológicas y Tecnológicas (IIByT-CONICET), Universidad Nacional de Córdoba, Córdoba, Argentina.

Running title: Microcapsules of soy genistein attenuate colitis

*Corresponding author: Prof. Dr. Silvia G. Correa, Inmunología, Departamento de Bioquímica Clínica, CIBICI (CONICET), Facultad de Ciencias Químicas, Universidad Nacional de Córdoba. Haya de la Torre y Medina Allende, 5000 Córdoba, Argentina

TE: 54 351 5353850#3105. e-mail: scorrea@fcq.unc.edu.ar

Abstract

We used water-soluble Chitosan obtained by Maillard reaction with glucosamine to microencapsulate soy genistein (Ge) and preserve its biological activity for oral administration. Release of Ge was pH dependent with a super Case II mechanism at pH 1.2 and an anomalous transport with non-Fickian kinetics at pH 6.8. Microencapsulated Ge retained its antioxidant properties *in vitro* and its daily administration to mice attenuated clinical signs of acute colitis, limited inflammatory reaction and reduced oxidative stress and tissue injury as well. Remarkably, after feeding microencapsulated Ge the production of IL-10 in colonic tissue was restored to levels of untreated controls. According to statistical multivariate analysis, this cytokine was the parameter with the highest influence on the inflammatory/oxidative status. Microencapsulation of Ge with derivatized Chitosan becomes an interesting alternative to develop therapeutic approaches for oxidative inflammatory diseases; our findings suggest that the soy isoflavone could be incorporated into any functional food for application in intestinal inflammation.

Keywords: genistein; Chitosan; microcapsules; inflammation; oxidative stress ; food

1. Introduction

In biological systems, production of reactive oxygen (ROS) and nitrogen (RNS) species is common and physiological scavenging activity keeps the balance between oxidation and antioxidation [1]. Excess of ROS and RNS may saturate the antioxidant machinery leading to chronic injury as described in inflammatory bowel diseases (IBD), where pro-inflammatory cytokines and oxidative reactions affect the redox equilibrium within the gut mucosa [1-3]. Accordingly, both IBD patients and mice with intestinal inflammation show higher levels of ROS in mucosal tissues [4]. Thus, the development of antioxidant strategies to restore intestinal homeostasis is critical and nowadays, therapeutic alternatives with biologic agents that either stimulate local production of anti-inflammatory molecules or affect the redox balance are intensely evaluated [3]. Flavonoids are natural compounds with phenolic groups that can accept electrons to form phenoxyl radicals, disrupting oxidation reactions in cellular components [5]. Among them, genistein (Ge), a phytoestrogen found primarily in soy products, has received wide attention due to its many biological activity such as binding to estrogen receptors [6], inhibition of tyrosine kinases [7], activation of endothelial nitric oxide synthase (eNOS), and production of defensins [8,9]. Moreover, it has been shown that the intake of 600 mg/kg Ge reduces inflammation, downregulates cytokine expression and improves colonic permeability in mice challenged with dextran sulfate sodium (DSS) [10], supporting an effective modulatory activity of Ge in intestinal mucosa.

Flavonoids in foods of natural origin are found as esters, glycosides or polymers that become partially hydrolyzed by the microbiota in the intestinal lumen, producing substances of smaller size less active and reducing the absorption efficiency. Additionally, flavonoids and other natural bioactive compounds are chemically

unstable, and susceptible to oxidative degradation particularly when exposed to oxygen, light, moisture, heat, and food processing conditions that may also affect their nutraceutical value [11-13]. Encapsulation systems as carriers of bioactive compounds can be useful tools to preserve their biological activity for oral administration [14]. Microencapsulation and nanoencapsulation are two important technological alternatives with several advantages to improve the functionality of the products. Most of the materials used for encapsulation are polymers of carbohydrates, proteins, lipids and other organic and inorganic materials that must be approved as "generally recognized as harmless" (GRAS) materials [15]. Several traditional techniques such as spray drying, freeze drying, extrusion, electrospinning, and coacervation are standard for encapsulating bioactive compounds [16], and recently, there has been growing interest in nanoscale delivery systems for bioactive compounds such as nanoparticles of biopolymers, nanohydrogels, neosomes, bilosomes, phytosomes, nanofibers, and flower-like porous lactose particles [17]. Specifically, for oral delivery of anti-inflammatory drugs, nanocarriers of functionalized mesoporous silica or multi-laminated metal hydroxide have been designed [18,19]. Herein, to preserve the antioxidant potential of Ge, we prepared microcapsules (MCs) with glucosamine water-soluble Chitosan derivative (WSChitosan) [20] by spray drying, a technique widely used due to its low cost that offer the possibility of continuous production of tailor-made particles for specific functions and needs of food industry [21]. Our findings show that microencapsulated Ge maintained its antioxidant properties *in vitro*. The daily oral administration of Ge using this delivery system blocked the inflammatory reaction in DSS colitis, limiting both tissue injury and oxidative stress. Remarkably, the flavonoid restored the production of IL-10, a critical mediator of the mucosal homeostasis.

2. Materials and Methods

2.1. Reagents

Chitosan MW 583 kDa (78% deacetylated), glucosamine hydrochloride (GAHC), nitrotetrazolium blue chloride (NBT), hydroxylamine hydrochloride (HAHC), 2-Deoxy-D-ribose (DoR), methionine, riboflavin, trichloroacetic acid (TCA), p-nitrophenyl-2-acetamido-β-glucopyranoside, citric acid, hexadecyl trimethyl ammonium bromide, sodium tripolyphosphate (TPP), aglycone Genistein (Ge) and fluorescein isothiocyanate (FITC) were obtained from Sigma-Aldrich (MO). Thiobarbituric acid (TBA) and ethylenediaminetetraacetic (EDTA) were provided by Merck (Germany); monobasic potassium phosphate (KH_2PO_4), sodium chloride (NaCl), sodium hydroxide (NaOH), potassium chloride (KCl), sodium bicarbonate ($NaHCO_3$), ascorbic acid, hydrogen peroxide (H_2O_2), hydrochloride acid (HCl), ferric chloride ($FeCl_3$), and glacial acetic acid (CH_3COOH) were from Cicarelli (Argentina). Dimethyl sulfoxide (DMSO) was from Biopack (Argentina). Bradford reagent was from Bio-Rad (USA) and 3,3',5,5' tetramethylbenzidine (TMB) was provided by BD Biosciences (USA). Dextran sulfate sodium (DSS) was kindly provided by Dextran Products Limited (Canada). Aqueous solutions were prepared with ultrapure water.

2.2. Mice

Six- to eight-week-old female C57BL/6 (B6) mice were used in these studies. Animals were maintained in specific pathogen-free conditions, housed in collective cages at 22 ± 1°C under a 12-h light/dark cycle (lights on at 7:00 a.m.) with free access to laboratory chow and drinking water. Animal experiments were approved by and conducted in accordance with guidelines of the Committee for Animal Care and Use of the Facultad

de Ciencias Químicas, Universidad Nacional de Córdoba (Approval N^{o} HCD 15-09-69596). Our animal facility obtained NIH animal welfare assurance (Assurance N^{o} A5802-01, Office of Laboratory Animal Welfare, NIH, Bethesda, MD, USA).

2.3. Preparation of water-soluble Chitosan derivative by Maillard reaction

Water-soluble derivatized Chitosan (WSChitosan) was obtained by Maillard reaction between Chitosan with glucosamine hydrochloride as described by Vanden Braber et al. [20].

2.4. Spray-Drying microencapsulation of Ge in WSChitosan

Microcapsules (MCs) with Ge were obtained as described by Vanden Braber et al. [22]. Ge was added to the shell material solution at 5% (w/w) of the biopolymer. Working conditions such as inlet temperature, liquid flow, aspiration rate and compressed spray air flow were set at 130 °C, 4 mL/min, 100% and 0.67 m^3/h, respectively. Empty MCs were prepared without Ge in the mixture to dry. Powders obtained after spray-drying were stored at -20 °C until analyzed.

2.5. Microencapsulation Efficiency

Microencapsulation efficiency (ME) was analyzed as described by Vanden Braber et al. [22]. To determine Ge content, we evaluated absorbance at 262 nm; ME, defined as percentage of Ge molecules in the core in relation to its total (core + surface) concentration, was calculated using equation (1) [23].

$$ME\ (\%) = \left([Ge]_I / [Ge]_T\right) \times 100 \quad (1)$$

where $[Ge]_I$ and $[Ge]_T$ are the Ge concentration inside and total in MCs, respectively; inner content was calculated by subtracting the total and outer content.

2.6. MCs morphology

Morphology and size distribution of spray-dried MCs were evaluated by scanning electronic microscopy (SEM) with a ZEISS SIGMA VP Field Emission Scanning Electron Microscope (FE-SEM) (ZEISS, Germany), using an acceleration voltage of 5 kV. MCs were fixed in stubs containing a double-faced adhesive metallic tape and coated with gold in a CED 010 vacuum evaporator (Balzers Union, Liechtenstein).

2.7. Release assays in simulated gastrointestinal digestion conditions

Ge release was studied for 48 h to simulate extended release in gastrointestinal conditions using an orbital shaker at a rotational speed of 150 rpm and 37°C as previously described [24,25]. We used 125 mM NaCl, 7mM KCl, 45 mM $NaHCO_3$, 0.1 N HCl at pH 1.2 to simulate the gastric fluid conditions (first 2.5 h) and 50 mM KH_2PO_4; 22.4 mM NaOH at pH 6.8 to simulate intestinal fluid conditions (the rest of the assay time).

Release profiles were fitted according to the mathematical model of Korsmeyer-Peppas equation (2) [26]. (2)

$$\frac{Ge_t}{Ge_\infty} = K_K t^n$$

In this equation, Ge_t/Ge_∞ is the fraction of Ge released at time t, K_K is the Korsmeyer-Peppas constant that incorporates structural and geometric characteristics, and n is a diffusional exponent that depends on the release mechanism and geometry of the tested system.

2.8. Hydroxyl radical scavenging activity assay

Hydroxyl radical ($HO^{\bullet}$) scavenging effect of MCs with Ge, empty MCs and pure Ge was determined as described [27]; the colored adduct was measured at 532 nm and the % of scavenging activity (SA) was calculated with equation (3):

$$SA\,(\%) = \left(1 - A_X / A_0\right) \times 100 \qquad (3)$$

A_0 is the absorbance of the control and A_X is the absorbance with MCs samples.

Trolox was used as antioxidant reference. The trolox equivalent activity (TEAC) was determined using a standard curve.

2.9. Superoxide radical scavenging activity assay

Scavenging of superoxide radical ($O_2^{\bullet -}$) of MCs with Ge, empty MCs and pure Ge was performed as described [27]; reduced NBT was measured at 560 nm and scavenging activity of $O_2^{\bullet -}$ was calculated with equation 3.

2.10. Biodisponibility studies

For biodisponibility studies, empty MCs were labeled with FITC as previously [28]; C57BL/6 mice were fed 200 µL empty MCs-FITC in 0.25% (v/v) acetic acid and 4-6 h later, duodenum, jejunum, ileum and colon from identical anatomical positions were removed; luminal content of each section was collected and centrifuged at 1,000 rpm; supernatants were used by flow cytometry; 100,000 fluorescent events were acquired on a FACSCanto (BD Pharmingen) and analyzed using FlowJo software (Tree Star, Inc.). As fluorescence negative controls, mice received unlabeled empty MCs in 0.25% (v/v) acetic acid.

2.11. Induction and assessment of experimental colitis

The DSS model is a robust, well established model that has been used to screen potential drug candidates and to investigate their mechanism of action [29]. Mice were randomly divided into four groups (n = 3-4 each): normal group (Control), control colitis group (DSS), DSS fed three times/day 1 mg of MCs / 100 µL in 0.25% (v/v) acetic acid with Ge in order to reach a daily dose of 0.08 mg of Ge / mouse (DSS+MCGe group), and DSS fed three times / day 1 mg of empty MCs / 100 µL in 0.25% (v/v) acetic acid (DSS+ empty MCs). Experiments were performed twice. Animals were examined daily and the Disease Activity Index (DAI) that combines weight loss, stool consistency and bleeding was calculated as described [30, 31]. On day 10, animals were sacrificed and colon removed for further studies.

2.12. Cytokines

Colon segments were homogenized as previously [30,31]; supernatants were stored at -70°C for further analysis. Murine TNF-α and MCP-1 (BD Biosciences), IL-6 and IL-10 (BD Pharmingen) were evaluated with ELISA kits as specified by the manufacturers.

2.13. Myeloperoxidase Assay

Myeloperoxidase (MPO) activity was performed as previously [30,31]. Results were expressed in optical density/mg tissue.

2.14. Superoxide dismutase activity

SOD activity was determined as described previously [32]. Results were expressed as SOD units/mg protein (one SOD unit is the enzyme activity that inhibits 50% the NBT reduction).

2.15. Malonaldehyde production

Malonaldehyde production was determined as previously [32]. Results were expressed in μmoles of MDA/mg protein.

2.16. Histopathological analysis

Excised portions of the distal colon were fixed immediately in 4% w/v formaldehyde solution and embedded in paraffin. Next, 5 μm sections were mounted on glass slides, and deparaffinized. For histological analysis, slices were stained using standard H&E

techniques. Images were taken with a Nikon optical microscope (Nikon eclipse TE2000-U, USA).

2.17. Statistical analysis

Data were expressed as means ± SEM. Statistical differences between groups were determined by one-way analysis of variance followed by Tukey post-test. A value of $p<0.05$ was considered statistically significant. Multidimensional analysis was performed to assess inflammatory profiles within the various conditions studied. We performed standardization of 6 parameters (DAI, colon Length/Weight, IL-10, TNF-α, IL-6 and MCP-1), so that each parameter would contribute in similar manner to the final classification; mice with similar characteristics were grouped within clusters. Statistical analysis was performed using GraphPad Prism 4 software (GraphPad Software, San Diego, CA, USA) and Infostat version 2008 FCA UNC, Argentina [33].

3. Results and Discussion

3.1 Preparation and characterization of MCs

Herein, we microencapsulated soy Ge using WSChitosan obtained by Maillard reaction as wall material, as we found previously that Chitosan derivatives kept functional properties of native polymer [20, 22]. Microencapsulation was performed by spray drying, an efficient and economical method [34] that has been successfully used with Chitosan as encapsulating material in food industry to protect several sensitive products [35, 36]. Morphology of MCs loaded with Ge (MCGe) assessed by SEM revealed predominantly spherical shape with a smooth surface (Fig. 1A and B). Collapsed aspect

was related to the intensive evaporation at the surface of each droplet, at the moment of mixing the air with the atomized liquid. Mean particle diameter was 2.62 μm (Fig. 1C), ranging from 1 to 4.63 μm [37].

ME (%) performed by exhaustive extraction showed that 78±5% of total Ge content was inside the particle, supporting the suitability of the wall material selected [38]. For *in vivo* experiments, doses were calculated considering the total content, which was 2.30±0.20% (w/w). Ge release *in vitro* followed a biphasic pattern, with an initial burst in simulated gastric conditions and a sustained release after 45.5 h under simulated intestinal conditions (Fig. 1D), indicating a release mechanism dependent on the pH. Data from Ge release in simulated gastrointestinal conditions were fitted with the Korsmeyer-Peppas equation (2). At pH 1.2, we found a release exponent (n) value of 0.94 and a regression coefficient (R^2) of 0.99, which matches with a super Case II transport type mechanism involving simultaneous contributions from dissolution, relaxation of the polymeric chain, erosion and swelling of Chitosan. During the first 4.5 h at pH 6.8, MCs presented an anomalous non-Fickian transport with R2 and n value of 0.96 and 0.67, respectively, corresponding to coupled diffusion/polymer relaxation, as described for indomethacin release from Chitosan-nanoparticles [39] or MCs of alginate and 0.25% Chitosan [40]. Under extended simulated intestinal conditions, a sustained release was observed, with a maximum value of 40%. In this way, although the sudden release of Ge allowed to reach quickly an effective concentration, the prolonged release promoted a sustained concentration of Ge in the effective range.

To evaluate free radical scavenging activity (SA), a comparative analysis was made between pure Ge, Ge from MCs and Trolox as antioxidant control (Fig. 2). SA (%) of Ge from MCs was calculated as the difference between SA (%) of MCs with Ge and empty MCs (Fig. S1). From the slope ratio it can be deduced that empty MCs contribute

90% and 36% to the scavenging of $O_2^{\bullet-}$ and $HO^{\bullet}$ radicals, respectively. Similar results were shown in our previous work with MCs of WSChitosan derivative loaded with quercetin [22]. In terms of SA (%) of $HO^{\bullet}$ radical, both pure Ge and Ge from MCs reached a plateau at 5 μM; however Ge from MCs exhibited a slightly higher activity (Fig. 2A); for $O_2^{\bullet-}$ radical scavenging, Ge from MCs showed higher activity at all concentrations tested (Fig. 2B). We also calculated the Trolox equivalent antioxidant capacity (TEAC) for pure and MCGe (Fig. 2C); for both radicals, Ge from MCs presented higher TEAC values (μM), with 2 (for $HO^{\bullet}$) and 1.5 (for $O_2^{\bullet-}$) fold more activity than pure Ge. This may be due to the fact that MCs are a controlled release system that allows the reposition of Ge in the medium. Chitosan has not always been considered an appropriate wall material; Kumar et al. reported that it was not able to protect squalene from oxidation during storage [40]. In our experimental condition, SA of Ge in MCs was preserved and the potency enhanced as well. The finding is relevant as Ge could be highly potent in TEAC assays but less potent in *in vitro* tests [41]. On the other hand, many natural compounds possess radical scavenging/antioxidative effects in cell-free systems but these results do not necessarily indicate activity against the oxidative stress *in vivo* [42].

3.2. Assessment of *in vivo* biodisponibility of MCs

In the digestive system wall materials interact with the environment and their ability to sustain the cores allow controlled release of bioactives [43]. In agreement, Chitosan is widely selected for sustained-release preparations in the small intestine [44]. On the other hand, effective treatments of IBD require selective accumulation of therapeutic agents in the intestine. Here we evaluated the presence of MCs in luminal content of

mice fed MCs-FITC using flow cytometry. Fig. S2 shows our gate strategy (A) and fluorescent particles in the luminal content of different gut sections (B). After 4 h of feeding, fluorescent particles were detected mainly in the small gut (>90%) with only 1% reaching the colon; in contrast 6 h after oral administration, around 30% of MCs-FITC was found in the colon, a main target in IBD. No fluorescence was detected in the colon of mice fed unlabeled MCs (data not shown). Accordingly, using fluorescently-labelled Chitosan–hypromellose MCs and multispectral small animal imaging, Ma et al. found higher colonic fluorescent intensity 8-24 h after oral administration, demonstrating the 'guarding' effect of Chitosan–hypromellose MCs during the transit along the gastrointestinal tract [45].

3.3. MCGe attenuates inflammatory response in DSS-induced colitis

Intestinal inflammation strongly correlates with oxidative stress; considering the sustained release of Ge in simulated intestinal environment (Fig. 1D), the strong antioxidant activity of MCGe (Fig. 2A and B) and the acceptable accumulation of MCs in colon after oral administration (Fig. S2B), we hypothesized that MCs could represent an efficient delivery platform of Ge for targeted treatment of intestinal inflammation. We used the acute murine model of DSS-colitis that recapitulates many clinical findings associated with human ulcerative colitis. As can be seen, mice treated with 3% DSS developed colitis on day 5, and progressively worsened until day 8, when they reached the highest DAI (Fig. 3); in contrast, daily oral administration of 0.08 mg Ge improved clinical signs and decreased DAI values. In agreement, natural antioxidants as 6-gingerol, ascorbic acid and *Sasa quelpaertensis* leaf extracts were able to suppress induction of ulcerative colitis via antioxidant and anti-inflammatory activities [46-48].

The administration of MCGe also prevented colon shortening induced by DSS (Fig. S3A and B). On day 10 colon sections of DSS group stained with H&E showed marked signs of inflammation, interstitial edema, epithelial erosion and abundant number of inflammatory cells in the lamina propria (Fig. 4B); with daily MCGe administration, histopathological signs were almost absent with lack of leukocyte infiltration (Fig. 4C), and tissue features similar to control group (Fig. 4A); in DSS+MCs mice, colon histoarchitecture was relatively conserved according to the weak inflammatory response found in this group (Fig. 4D). Interestingly, mice treated with empty MCs showed a mild protective effect on days 6-8, possibly related to the antioxidant and anti-inflammatory bioactivities of WSChitosan derivatives [20, 22] and Chitosan itself [49]. Notably, MPO activity, a marker of neutrophil infiltration, augmented in DSS-induced colitis group (Fig. 4E) and was significantly reduced in MCGe and MCs mice with similar values to control group. The oral administration of both MCGe and MCs reduced significantly the production of pro-inflammatory cytokines IL-6 (Fig. 5A) and TNF-α (Fig. 5B) and the chemokine MCP-1 (Fig. 5C), that regulates migration and infiltration of monocytes/macrophages.

In terms of antioxidant actions *in situ*, SOD activity increased in colonic samples of DSS group (Fig. 6A); in striking contrast, mice treated with MCGe exhibited similar values to control group. Accordingly, supplementation of feeding diet with soy isoflavones reduced signs of colitis and exhibited antioxidant activity with increased expression of ZnCuSOD and glutathione peroxidases [50]. MCGe antioxidant ability was further confirmed by malonaldehyde (MDA) levels in tissue samples (Fig. 6B), where DSS+MCGe group presented similar values to control mice. Other reports have suggested that Ge has no effect in clinical signs of colitis while soy equol exacerbated

weight loss at the higher dose evaluated [51]. We found that non-encapsulated Ge was unable to mediate anti-oxidant and anti-inflammatory effects (Fig. S4); mice fed pure Ge developed severe colitis comparable to DSS group (A), with similar levels of MCP-1 (B), MPO (C) and SOD (D) activities and leukocyte infiltration (E). Together, differences in delivery system and Ge dose could explain dissimilar results, since using a similar daily dose, we found that pure Ge had no beneficial effect on the inflammatory and oxidative responses elicited by DSS. Remarkably, these findings confirmed that microencapsulation efficiently preserved the biological properties of Ge.

3.4. MCGe restores master regulatory cytokine in DSS-induced colitis

As shown in Fig. 5D, MCGe stimulated the recovery of the master regulatory cytokine IL-10 to levels found in control group. Remarkably, the production of this key anti-inflammatory mediator was a selective effect of MCs loaded with Ge, as IL-10 levels in mice fed empty MCs were similar to DSS group. This was an unexpected result as a diet with 600 mg Ge/kg alleviated DSS-caused colonic injury and improved tight junction protein expression in Caco cells without modifying IL-10 production [10]. To confirm the relevance of our finding we performed Principal Component Analysis (PCA) to describe the inflammatory status of treated (MCs+DSS and MCGe+DSS) and untreated (DSS and control) groups. We considered the following parameters: DAI, IL-10, TNF-α, IL-6, MCP-1, and Length/Weight of colon. As can be seen (Fig. 7A), Principal Components 1 (PC1) and 2 (PC2) explained 82.5% of total variability of the data; Analysis of each parameter showed that IL-10 was the variable with the highest influence on PC1 configuration for groups (data not shown); interestingly, control and DSS+MCGe mice that presented similar values of IL-10 in colonic tissue clustered together (Fig. 7A), supporting the recovery of this master regulator upon treatment with

Ge. In agreement, Zhikang Capsule, a traditional Chinese medicine widely used for IBD therapy, effectively promoted the production of IL-10, limited neutrophil influx and MPO activity and restored SOD and MDA to control values [52]. The minimal spanning tree (MST) depicted in Fig. 7B, where 100% of the data variability was taken into account, evidence the higher integration between control and DSS+MCGe mice, compared with DSS+MCs and DSS groups. Additionally, oxidative parameters (MPO and SOD activities and MDA production) were included in multivariate analysis and correlation coefficients were calculated (Fig. 7C). Interestingly, we found a negative correlation of IL-10 with all parameters studied that was significant with DAI and MCP-1 values. Accordingly, IL-10 interacts with the cellular machinery inhibiting ROS production, which in turn decreases NF-κB activity and the expression of inflammatory cytokines [53]. Moreover, in a model of *S. japonicum* infection, Ge decreased NF-κB signaling, and subsequently reduced MCP-1, TNF-α and IL-10 production [54]. The concept that IL-10 could act as an antioxidant blocking the release of ROS provides new pathways to understand the redox/oxidant perturbation during the evolution of inflammatory states.

4. Conclusions

Conventional therapies for treating IBD are usually associated with complications or side effects; therefore, development of safer therapeutic options is essential. Here we demonstrated that the delivery of Ge in MCs of WSChitosan produced drastic reduction of clinical parameters in DSS colitis, attenuating tissue injury and normalizing both inflammatory (IL-6, TNF-α, MCP-1) and oxidative (SOD, MDA, MPO) markers.

Remarkably, only those mice treated with MCGe restored the production of IL-10 to homeostaic levels. The targeted effect involved both IL-10 and redox/oxidant axis. The pivotal role of IL-10 in MCGe mice was confirmed with multivariate analysis, where IL-10 turned out to be the variable with highest influence on PC1 configuration for control and MCGe groups. Together, our data show that the delivery platform of the isoflavone described here could be considered an interesting alternative for therapeutic approach to treat intestinal inflammatory conditions.

Acknowledgements

We would like to thank Paula Icely, Pilar Crespo, Paula Abadie and Fabricio Navarro for excellent technical assistance. This work was supported by the Agencia Nacional de Promoción Científica y Tecnológica (FONCYT) [grant numbers PICT 0117 2016 and PICT 1068 2013]; Consejo Nacional de Investigaciones Científicas y Tecnológicas (CONICET) and Secretaría de Ciencia y Tecnología de la Universidad Nacional de Córdoba (SECYT-UNC). Dextran sulphate sodium was a gift of George Usher, Dextran Products Limited (Canada). Fellows were funded by CONICET (NVB and INN); LB, CP, FNN, MM, SGC are career members of CONICET.

Conflicts of interest

None.

References

[1] Alfadda AA, Sallam RM. Reactive oxygen species in health and disease. J Biomed. Biotechnol 2012; 2012:936486.

[2] Zhu H, Li YR. Oxidative stress and redox signaling mechanisms of inflammatory bowel disease: Updated experimental and clinical evidence. Exp Biol Med 2012; 237:474–80.

[3] Katsanos KH. Papadakis, K.A. Inflammatory Bowel Disease: Updates on Molecular Targets for Biologics. Gut Liver 2017;11:455-63.

[4] Chong WC, Shastri MD,Eri R. Endoplasmic Reticulum Stress and Oxidative Stress: A Vicious Nexus Implicated in Bowel Disease Pathophysiology. Int J Mol Sci 2017; 18:4.

[5] Pandey KB, Rizvi SI. Plant polyphenols as dietary antioxidants in human health and disease. Oxid Med Cell Longev2009; 2:270–78.

[6] Kim H, Peterson TG, Barnes S. Mechanisms of action of the soy isoflavone genistein: emerging role for its effects via transforming growth factor beta signaling pathways. Am J Clin Nutr 1998;68: 1418S-25S.

[7] Natarajan K, Manna SK,Chaturvedi MM, Aggarwal BB. Protein tyrosine kinase inhibitors block tumor necrosis factor-induced activation of nuclear factor-κB, degradation of IκBα, nuclear translocation of p65, and subsequent gene expression. Arch Biochem Biophys 1998;352: 59–70.

[8] Babu PV, Si H, Fu Z, Zhen W, Liu D. Genistein prevents hyperglycemia-induced monocyte adhesion to human aortic endothelial cells through preservation of the cAMP signaling pathway and ameliorates vascular inflammation in obese diabetic mice. J Nutr 2012;142: 724-30.

[9] Srisomboon Y, Poonyachoti S, Deachapunya C. Soy isoflavones enhance β-defensin synthesis and secretion in endometrial epithelial cells with exposure to TLR3 agonist polyinosinic-polycytidylic acid. Am J Reprod Immunol 2017;78:4.

[10] Zhang R, Xu J, Zhao J, Chen Y. Genistein improves inflammatory response and colonic function through NF-κB signal in DSS-induced colonic injury. Oncotarget 2017; 8: 61385-392.

[11] Hu D, Xu Y, Xie J, Sun C, Zheng X, Chen W. Systematic evaluation of phenolic compounds and protective capacity of a new mulberry cultivar J33 against palmitic acid-induced lipotoxicity using a simulated digestion method. Food Chem 2018; 258: 43-50.

[12] Ross JA, Kasum CM. Dietary flavonoids bioavailability, metabolic effects, and safety. Annu Rev Nutr 2002;2: 19–34.

[13] Williamson G, Manach C. Bioavailability and bioefficacy of polyphenols in humans. II. Review of 93 intervention studies. Am J Clin Nutr 2005;81:243S–5S.

[14] Zheng Li, Hong Jiang, Changmou Xu, Liwei Gu. A review: Using nanoparticles to enhance absorption and bioavailability of phenolic phytochemicals. Food Hydrocolloids 2015; 43:153-64.

[15] Robin AL, Sankhla D. European legislative framework controlling the use of food additives. In: Saltmarsh M, editor. Essential guide to food additives, Cambridge: RSC Publishing; 2013, p. 44–53.

[16] de Souza Simões L, Madalena DA, Pinheiro AC, Teixeira JA, Vicente AA, Ramos ÓL. Micro- and nano bio-based delivery systems for food applications: In vitro behavior. Adv Colloid Interface Sci 2017; 243: 23–45.

[17] McClements DJ. Nanoscale Nutrient Delivery Systems for Food Applications: Improving Bioactive Dispersibility, Stability, and Bioavailability. J Food Sci 2015;80: 1602-11.

[18] Lee CH, Lo LW, Mou CY, Yang CS. Synthesis and Characterization of Positive-Charge Functionalized Mesoporous Silica Nanoparticles for Oral Drug Delivery of an Anti-Inflammatory Drug. Adv Funct Mater 2008;18: 3283-92.

[19] Kankala RK, Kuthati Y, Sie HW, Shih HY, Lue SI, Kankala S et al. Multi-laminated metal hydroxide nanocontainers for oral-specific delivery for bioavailability improvement and treatment of inflammatory paw edema in mice. J Colloid Interface Sci 2015; 458: 217–28.

[20] Vanden Braber NL, Díaz VergaraLI, Morán Vieyra FE, Borsarelli CD, Yossen MM, Vega JR et al. Physicochemical characterization of water-soluble chitosan derivatives with singlet oxygen quenching and antibacterial capabilities. Int J Biol Macromol 2017;102: 200-07.

[21] Desai KGH, Park HJ. Recent developments in microencapsulation of food ingredients. Drying Technol 2005; 23: 1361-94.

[22] Vanden Braber NL, Paredes AJ, Rossi YE, Porporatto C, Allemandi DA, Borsarelli CD et al. Controlled release and antioxidant activity of chitosan or its

glucosamine water-soluble derivative microcapsules loaded with quercetin. Int J Biol Macromol 2018;112: 399-404.

[23] McNamee BF, O'Riordan ED, O'Sullivan M. Effect of partial replacement of gum arabic with carbohydrates on its microencapsulation properties. J Agric Food Chem 2001;49: 3385–88.

[24] Harris R, Lecumberri E, Mateos-Aparicio I, Mengíbar M, Heras A. Chitosan nanoparticles and microspheres for the encapsulation of natural antioxidants extracted from Ilex paraguariensis. Carbohydr Polym 2011; 84:803–06.

[25] Guazelli CF, Fattori V, Colombo BB, Georgetti SR, Vicentini FT, Casagrande R et al. Quercetin-Loaded Microcapsules Ameliorate Experimental Colitis in Mice by Anti-inflammatory and Antioxidant Mechanisms. J Nat Prod 2013;76: 200–08.

[26] Ferrero C, Massuelle D, Doelker E. Towards elucidation of the drug release mechanism from compressed hydrophilic matrices made of cellulose ethers. II. Evaluation of a possible swelling-controlled drug release mechanism using dimensionless analysis. J Control Release 2010;141: 223-33.

[27] Boiero ML, Mandrioli M, Vanden Braber N, Rodriguez-Estrada MT, García, NA, Borsarelli CD et al. Gum arabic microcapsules as protectors of the photoinduced degradation of riboflavin in whole milk. J Dairy Sci 2014;97: 5328-36.

[28] Qaqish R, Amiji M. Synthesis of a fluorescent chitosan derivative and its application for the study of chitosan–mucin interactions. Carbohydr Polym 1999;38; 99–107.

[29] Chassaing B, Aitken JD, Malleshappa M, Vijay-Kumar M. Dextran sulfate sodium (DSS)-induced colitis in mice. Curr Protoc Immunol. 2014;104:Unit 15.25.

[30] Sena AA, Pedrotti LP, Barrios BE, Cejas H, Balderramo D, Diller A et al. Lack of TNFRI signaling enhances annexin A1 biological activity in intestinal inflammation. Biochem Pharmacol 2015;98: 422-31.

[31] Pedrotti LP, Sena AA, Rodriguez Galán MC, Cejas H, Correa SG. Intestinal mononuclear cells primed by systemic interleukin-12 display long-term ability to aggravate colitis in mice.Immunology 2017;150: 290-300.

[32] Liaudat AC, Bohl LP, Tolosa de Talamoni NG, Maletto B, Pistoresi-Palencia, MC, Picotto G. Oxidative stress, cell cycle arrest and differentiation contribute toward the antiproliferative action of BSO and calcitriol on Caco-2 cells. Anticancer Drugs 2014; 25: 810–18.

[33] Di Rienzo JA, Casanoves F, Balzarini MG, Gonzalez L, Tablada M, Robledo CW. Infostat, version 2008, Grupo InfoStat, FCA, Universidad Nacional de Córdoba, Argentina.

[34] Gharsallaoui A, Roudaut G, Chambin O, Voilley A, Saurel R. Applications of spray-drying in microencapsulation of food ingredients: An overview. Food Res Internat 2007;40: 1107–21.

[35] Berendsen R, Güell C, Ferrando M. Spray dried double emulsions containing procyanidin-rich extracts produced by premix membrane emulsification: effect of interfacial composition. Food Chem 2015; 178: 251-58.

[36] Gültekin-Özgüven M, Karadağ A, Duman Ş, Özkal B, Özçelik B. Fortification of dark chocolate with spray dried black mulberry (Morus nigra) waste extract encapsulated in chitosan-coated liposomes and bioaccessability studies. Food Chem 2016; 201: 205-12.

[37] Carneiro HCF, Tonon RV, Grosso CRF, Hubinger MD. Encapsulation efficiency and oxidative stability of flaxseed oil microencapsulated by spray drying using different combinations of wall materials. J Food Eng 2013; 115:443–51.

[38] Abul Kalam M, Khan AA, Khan S, Almalik A, Alshamsan A. Optimizing indomethacin-loaded chitosan nanoparticle size, encapsulation, and release using Box-Behnken experimental design. Int J Biol Macromol 2016;87: 329-40.

[39] Ghaffarian R, Herrero EP, Oh H, Raghavan SR, Muro S. Chitosan-Alginate Microcapsules Provide Gastric Protection and Intestinal Release of ICAM-1-Targeting Nanocarriers, Enabling GI Targeting In Vivo. Adv Funct Mater 2016; 26: 3382-93.

[40] Kumar LRG, Chatterjee NS, Tejpal CS, Vishnu KV, Anas KK, Asha KK et al. Evaluation of chitosan as a wall material for microencapsulation of squalene by spray drying: Characterization and oxidative stability studies. Int J Biol Macromol 2017;104:1986-95.

[41] Rüweler M, Anker A, Gülden M, Maser E, Seibert H. Inhibition of peroxide-induced radical generation by plant polyphenols in C6 astroglioma cells. Toxicol In Vitro 2008; 22: 1377-781.

[42] Aruoma OI. Methodological considerations for characterizing potential antioxidant actions of bioactive components in plant foods. Mutation Research 2003;523-524:9-20.

[43] Lee PS, Yim SG, Choi Y, Van Anh Ha T, Ko S. Physiochemical properties and prolonged release behaviours of chitosan-denatured β-lactoglobulin microcapsules for potential food applications. Food Chem 2012;134: 992-98.

[44] Shimono N, Takatori T, Ueda M, Mori M, Nakamura A. Multiparticulate chitosan-dispersed system for drug delivery. Chem Pharm Bull2003;51: 620-624.

[45] Ma GY, Fuchs AV, Boase NR, Rolfe BE, Coombes AG, Thurecht KJ. The in vivo fate of nanoparticles and nanoparticle-loaded microcapsules after oral administration in mice: Evaluation of their potential for colon-specific delivery. Eur J Pharm Biopharm 2015:94: 393-403.

[46] Ajayi BO, Adedara IA, Farombi EO. Pharmacological activity of 6-gingerol in dextran sulphate sodium-induced ulcerative colitis in BALB/c mice. Phytother Res 2015;29: 566-72.

[47] Yan H, Wang H, Zhang X, Li X, Yu J. Ascorbic acid ameliorates oxidative stress and inflammation in dextran sulfate sodium-induced ulcerative colitis in mice. Int J Clin Exp Med 2015;8: 20245–253.

[48] Yeom Y, Kim Y. The Sasa quelpaertensis Leaf Extract Inhibits the Dextran Sulfate Sodium-induced Mouse Colitis Through Modulation of Antioxidant Enzyme Expression. J Cancer Prev 2015;20: 136-46.

[49] Yuan G, Chen X, Li D. Chitosan films and coatings containing essential oils: The antioxidant and antimicrobial activity, and application in food systems. Food Res Int 2016; 89: 117-28.

[50] Wang B, Wu C. Dietary soy isoflavones alleviate dextran sulfate sodium-induced inflammation and oxidative stress in mice. Exp Ther Med 2017; 14:276-82.

[51] Sakai T, Furoku S, Nakamoto M, Shuto E, Hosaka T, Nishioka Y et al. Soy isoflavone equol perpetuates dextran sulfate sodium-induced acute colitis in mice. Biosci Biotechnol Biochem 2011;75: 593-95.

[52] Fei L, Xu K. Zhikang Capsule ameliorates dextran sodium sulfate-induced colitis by inhibition of inflammation, apoptosis, oxidative stress and MyD88-dependent TLR4 signaling pathway. J Ethnopharmacol 2016;192: 236-47.

[53] Dokka S, Shi X, Leonard S, Wang L, Castranova V. Rojanasakul Y. Interleukin-10-mediated inhibition of free radical generation in macrophages. Am J Physiol Lung Cell Mol Physiol 2001;280: L1196-202.

[54] Wan C, Jin F, Du Y, Yang K, Yao L, Mei Z et al. Genistein improves schistosomiasis liver granuloma and fibrosis via dampening NF-kB signaling in mice. Parasitol Res 2017; 116:1165-74.

Figure Legends

Figure 1. Morphology of MCGe and Ge release in gastrointestinal conditions. SEM microphotographs of spray-dried particles with Ge (acceleration voltage of 5 kV) (A and B). MCGe sizes (n=100) obtained with SEM (C). Released Ge in simulated gastrointestinal digestion assays (D). Results were expressed as means ± SEM. Experiments were made by duplicate.

Figure 2. Scavenging activity of MCGe. Percent scavenging activity of radicals HO• (A) and O_2•− (B) by MCGe (●), pure Ge (o) and trolox (■). Trolox equivalent antioxidant activity (TEAC) for radicals (C). Results were expressed as means ± SEM. Experiments were made by duplicate. Means with different letters, in the same column, are significantly different ($p < 0.05$).

Figure 3. Clinical resolution of DSS-colitis after treatment with MCGe. Mice from DSS, DSS+MCGe and DSS+empty MCs groups received 3% DSS for 5 days and drinking water for the next 5 days; mice from MCGe and MCs groups were fed three times/day 75 µL of a 1 mg MCs suspension/100 µL in 0.25 % (v/v) acetic acid; the daily dose of Ge was 0.08 mg/mouse. Control groups received daily the same volume of 0.25% acetic acid. All mice were evaluated daily during 10 days for clinical signs to

assess the Disease Activity Index (DAI); data are mean ± SEM (n = 3-4 animals/group). Experiments were made by duplicate. Different letters indicate significant differences between groups on the same day ($p < 0.05$).

Figure 4. Histopathological analysis of colon after treatment with MCGe. Sections obtained on day 10 after colitis induction were stained with H&E. Representative microphotographs from control (A), DSS (B), DSS + MCGe (C) and DSS + empty MCs (D) groups. Magnification: 400x. Colonic myeloperoxidase (MPO) activity per mg of tissue (E). Data are mean ± SEM (n= 3-4 animals per group). Experiments were made by duplicate. Different letters indicate significant differences between groups ($p < 0.05$).

Figure 5. Cytokines in colon of mice with DSS colitis after MCGe treatment. Cytokines (IL-6, TNF-α, MCP-1 and IL-10) were quantified by ELISA kits in tissue homogenates obtained at the end of the treatment (day 10). Data are mean ± SEM (n= 3-4 animals/group). Experiments were made by duplicate. Different letters indicate significant differences between groups ($p < 0.05$).

Figure 6. Oxidative stress in colon of mice with DSS colitis after MCGe treatment. Superoxide dismutase (SOD) activity (A) and malondialdehyde (MDA) (B) were evaluated in colon homogenates obtained at the end of the treatment (day 10). Data are mean ± SEM (n=3-4 animals/group). Experiments were made by duplicate. Different letters indicate significant differences between groups ($p < 0.05$).

Figure 7. Exploration of data variability and clustering in Ge treated and treated mice. Principal component analysis bi-plot graphs. Each mouse is represented by a dot and each explanatory and clustering variable used in the analysis is represented by a line. Eigenvalues are shown in parentheses next to each component (A). Representation

of the minimal spanning tree (MST) on the bi-plot graph (B); Spearman correlation coefficients; underlined values have significant correlation (C); P<0.05).

Supplementary Figure Legends

Figure S1. Percent scavenging activity of radicals $HO^{\bullet}$ (A) and $O_2^{\bullet -}$ (B) by (○) empty MCs and (●) MCGe.

Figure S2. Assessment of microcapsule biodisponibility in intestine. Mice (n=3) were fed 200 µL of empty MCs unlabeled or labeled with FITC; 4 or 6 h later the whole intestine was removed and the luminal content free of debris from identical sections of small intestine (duodenum, jejunum and ileum) and colon was evaluated for flow cytometry in mice from different groups. Gatting strategy (A); representative histograms were the proportion of fluorescent events in each section is depicted (B). Experiments were made by duplicate.

Figure S3. Morphology and Lenght / Weight colon ratio in different experimental groups. A) Representative photographs of colon at the end of the treatment in Control, DSS, DSS+ MCGe and DSS+ MCs groups; B) Lenght / Weight colon ratio (B). Data are mean ± SEM (n = 3-4 animals/group). Experiments were performed twice. Different letters indicate significant differences between groups ($p< 0.05$).

Figure S4. Evaluation of clinical signs of DSS colitis after treatment with unencapsulated Ge. Mice from DSS and DSS+Ge groups received 3% DSS for 5 days and drinking water for the next 5 days; mice from Ge groups were fed three times/day 75 µL of Ge in 0.25 % (v/v) acetic acid and the daily dose of Ge was 0.08 mg/mouse. Control groups received daily the same volume of 0.25% (v/v) acetic acid. All groups were evaluated daily during 10 days for clinical signs. Disease Activity Index (DAI) at the end of the treatment (A), MCP-1 level (B), colonic myeloperoxidase (MPO)

activity, (C) superoxide dismutase (SOD) activity (D) and representative H&E stained section (E). Data are mean ± SEM (n= 3-4 animals/group). Experiments were made by duplicate. Different letters indicate significant differences between groups ($p < 0.05$).

Highlights.

- We used a Chitosan soluble derivative to microencapsulate genistein.
- Microcapsules preserved genistein biological properties and reached colon upon feeding.
- Microencapsulated genistein reduced intestinal inflammation and tissue damage in mice.
- The observed effects were dependent on IL-10 production.
- Microencapsulated genistein could be incorporated in functional foods.

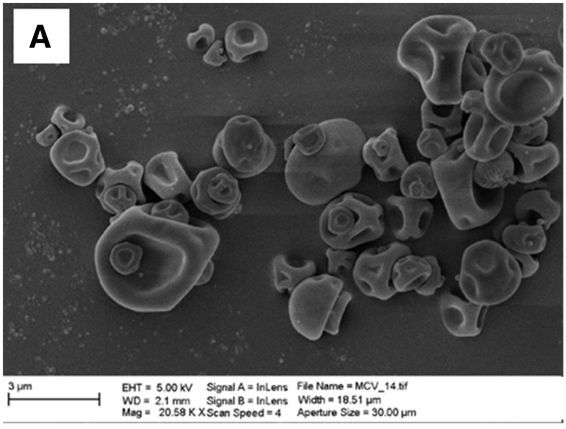

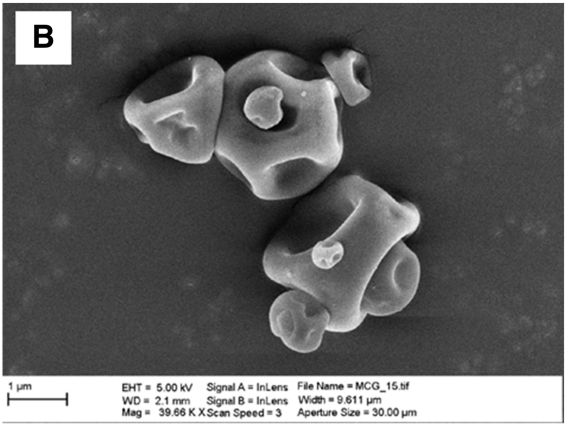

C. MCGe size from SEM.

Size (µm) of MCGe	
Mean	2.62±0.87
Max.	4.63
Min.	1.00

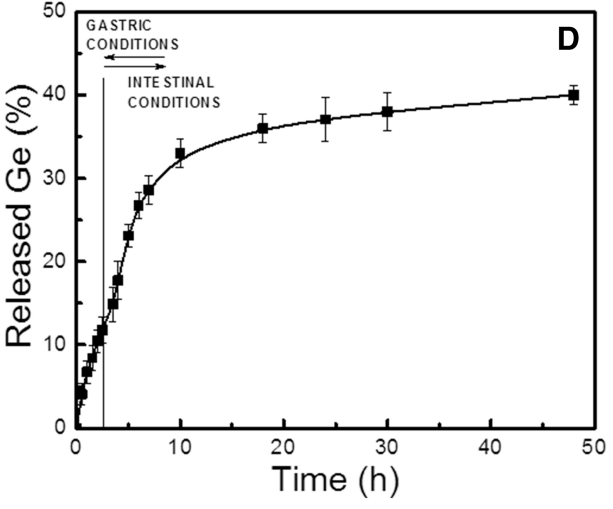

Figure 1

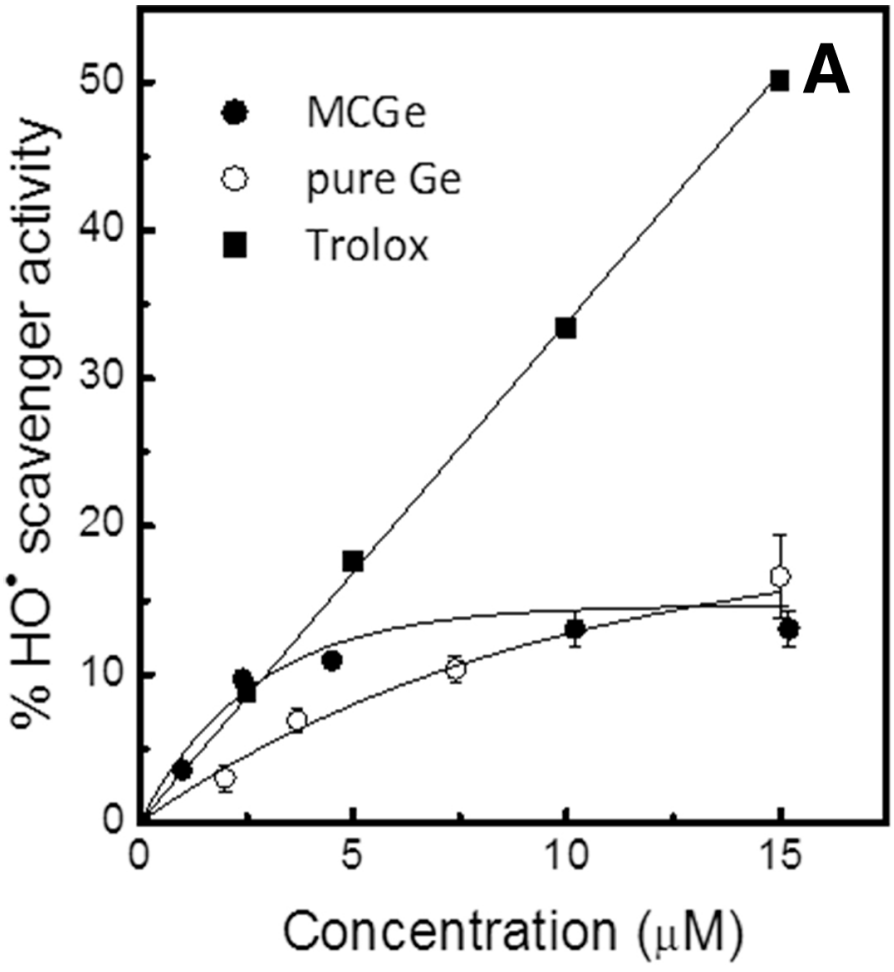

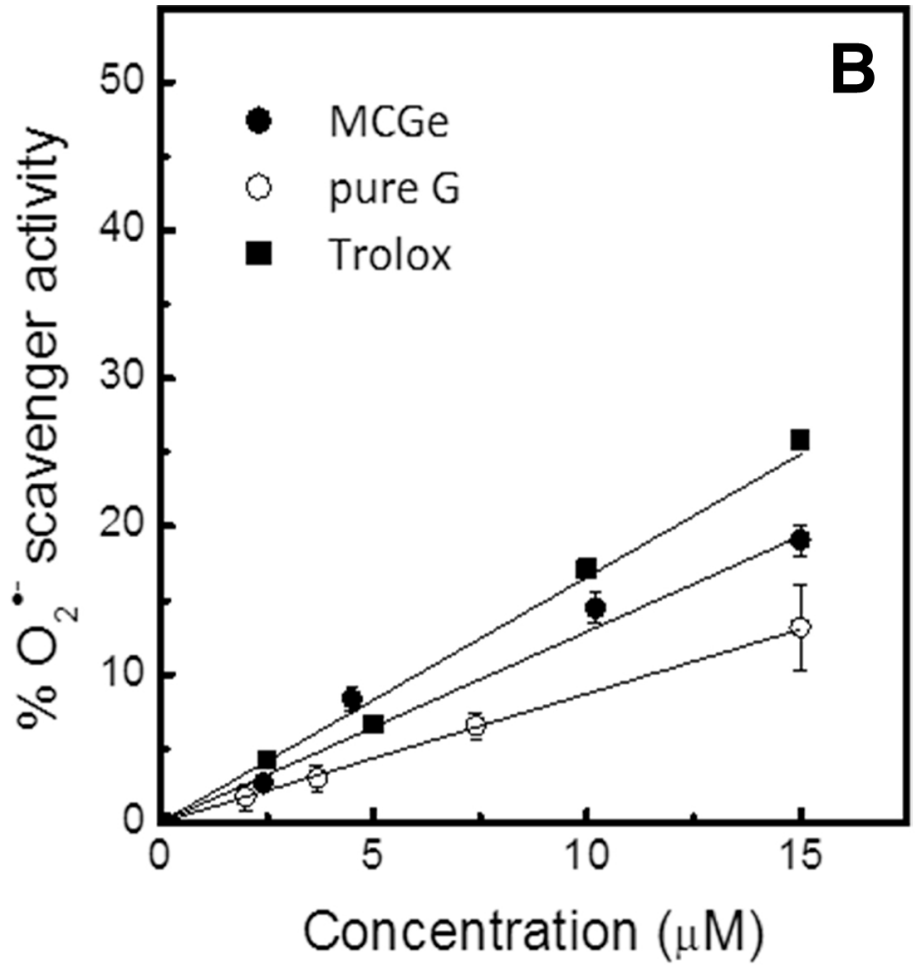

C. TEAC values (μM) for pure and microencapsulated Ge.

Antioxidant	TEAC (μmol L^{-1})	
	$HO^{\bullet}$	**$O_2^{\bullet-}$**
MCGe	0.87 ± 0.03^{b}	0.78 ± 0.02^{b}
pure Ge	0.42 ± 0.03^{a}	0.52 ± 0.01^{a}

Figure 2

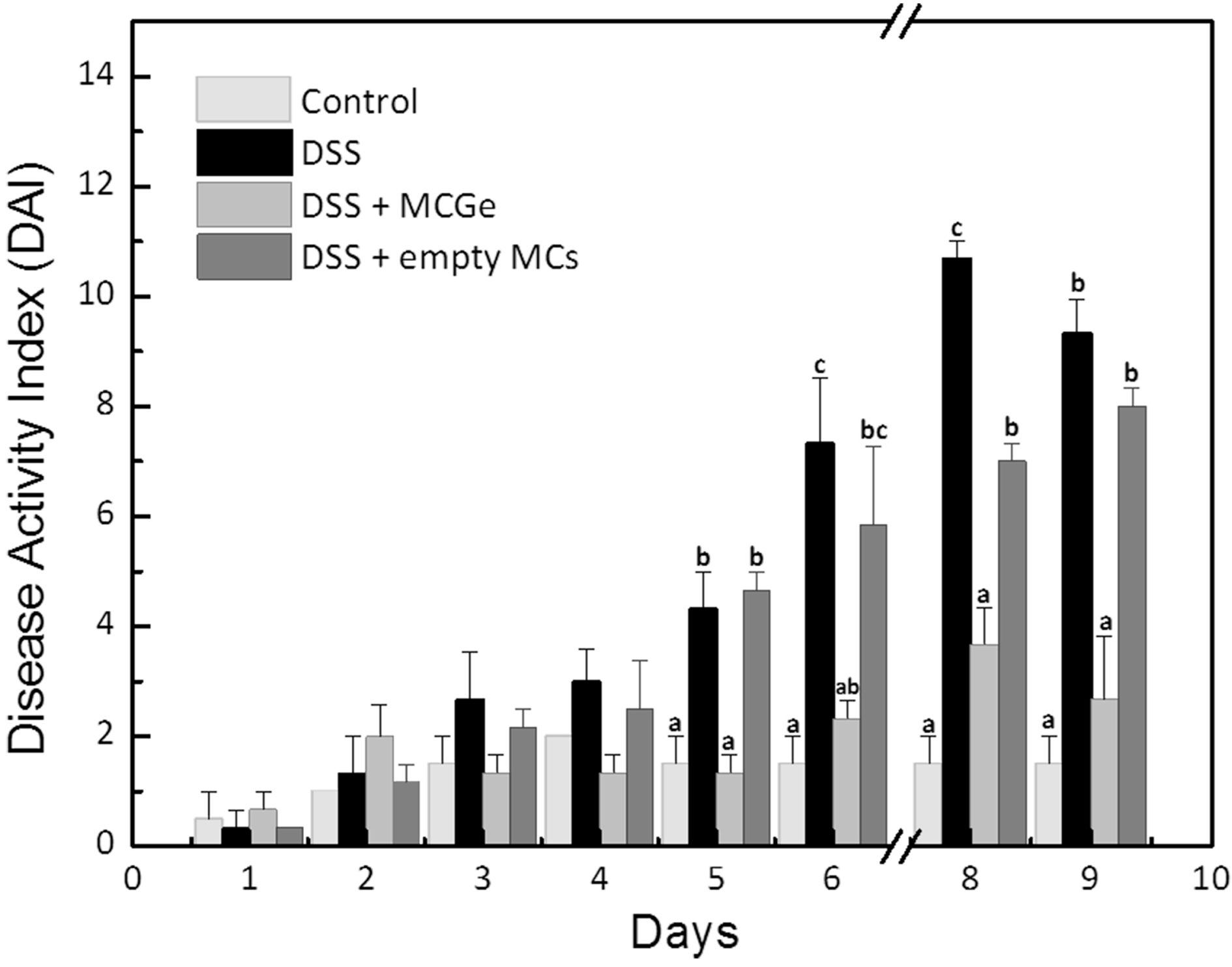
Control
DSS
DSS + MCGe
DSS + empty MCs
Disease Activity Index (DAI)
Days
0
2
4
6
8
10
12
14
0
1
2
3
4
5
6
8
9
10
a
b
c
ab
bc

Figure 3

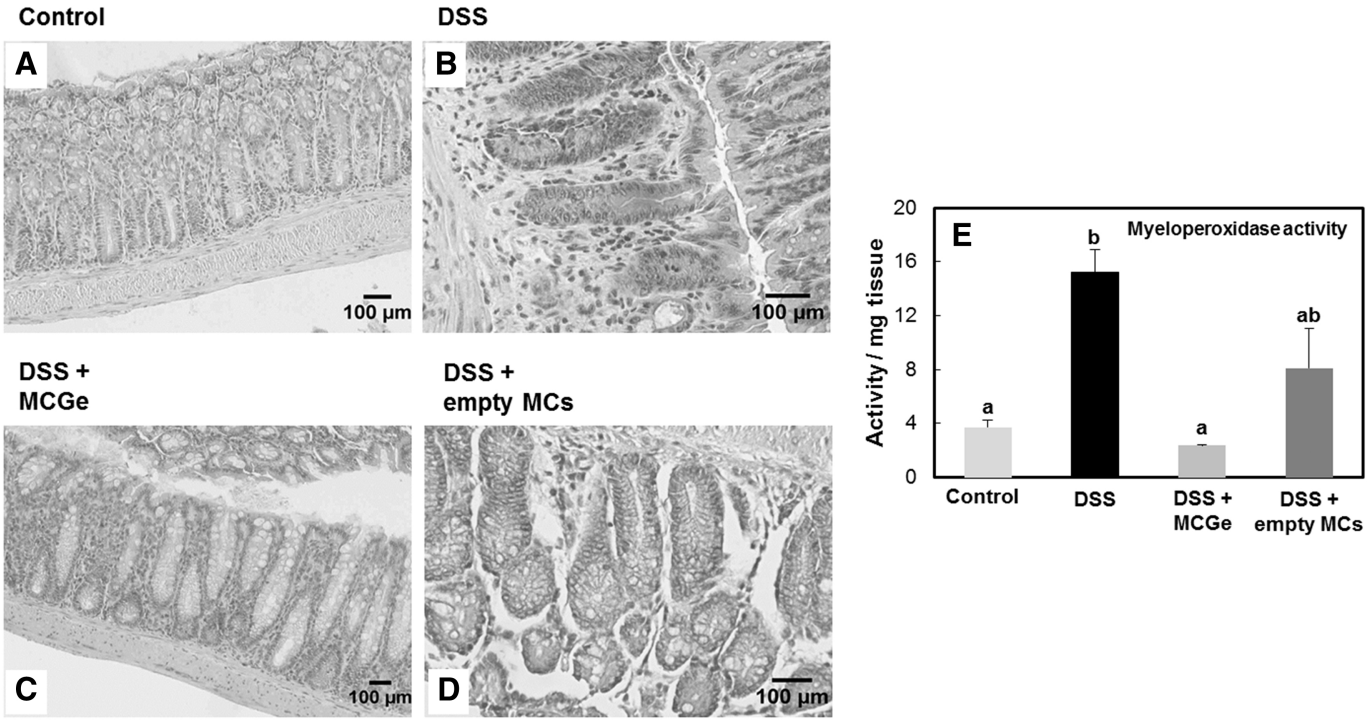
Control
A
100 µm
DSS
B
100 µm
DSS +
MCGe
C
100 µm
DSS +
empty MCs
D
100 µm
E
Myeloperoxidase activity
Activity / mg tissue
20
16
12
8
4
0
a
b
a
ab
Control
DSS
DSS +
MCGe
DSS +
empty MCs

Figure 4

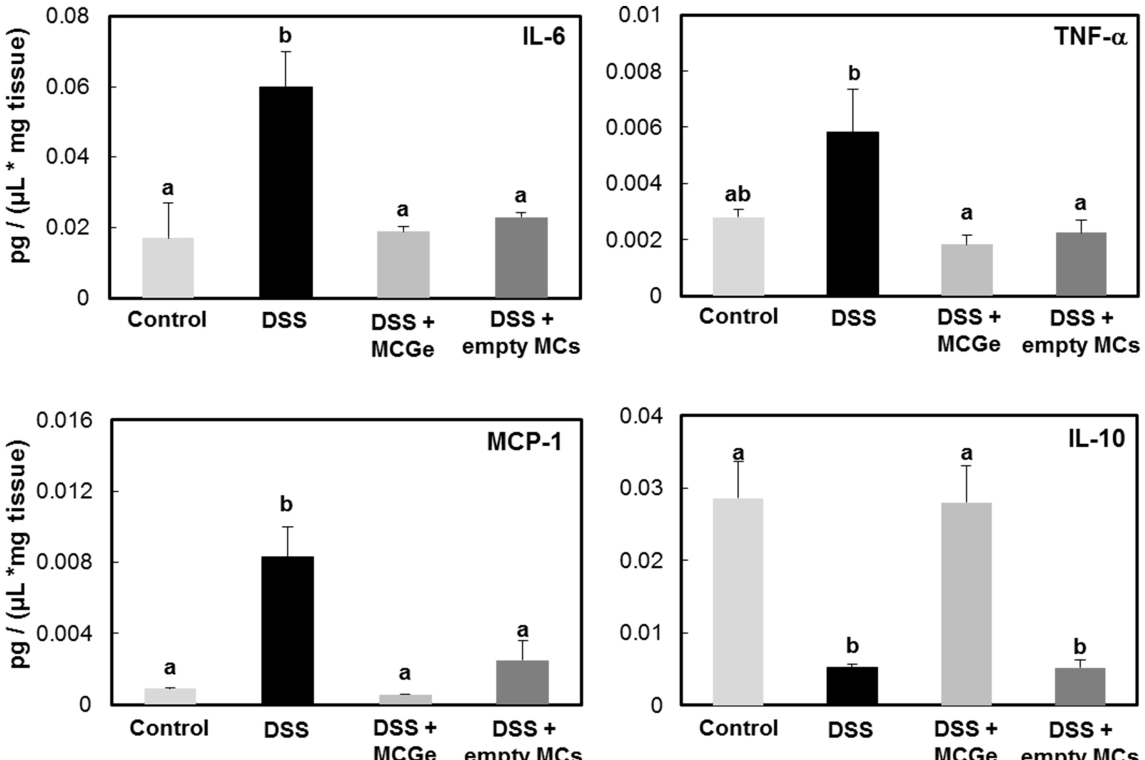
IL-6
pg / (µL * mg tissue)
0.08
0.06
0.04
0.02
0
a
b
a
a
Control
DSS
DSS + MCGe
DSS + empty MCs
TNF-α
0.01
0.008
0.006
0.004
0.002
0
ab
b
a
a
Control
DSS
DSS + MCGe
DSS + empty MCs
MCP-1
pg / (µL *mg tissue)
0.016
0.012
0.008
0.004
0
a
b
a
a
Control
DSS
DSS + MCGe
DSS + empty MCs
IL-10
0.04
0.03
0.02
0.01
0
a
b
a
b
Control
DSS
DSS + MCGe
DSS + empty MCs

Figure 5

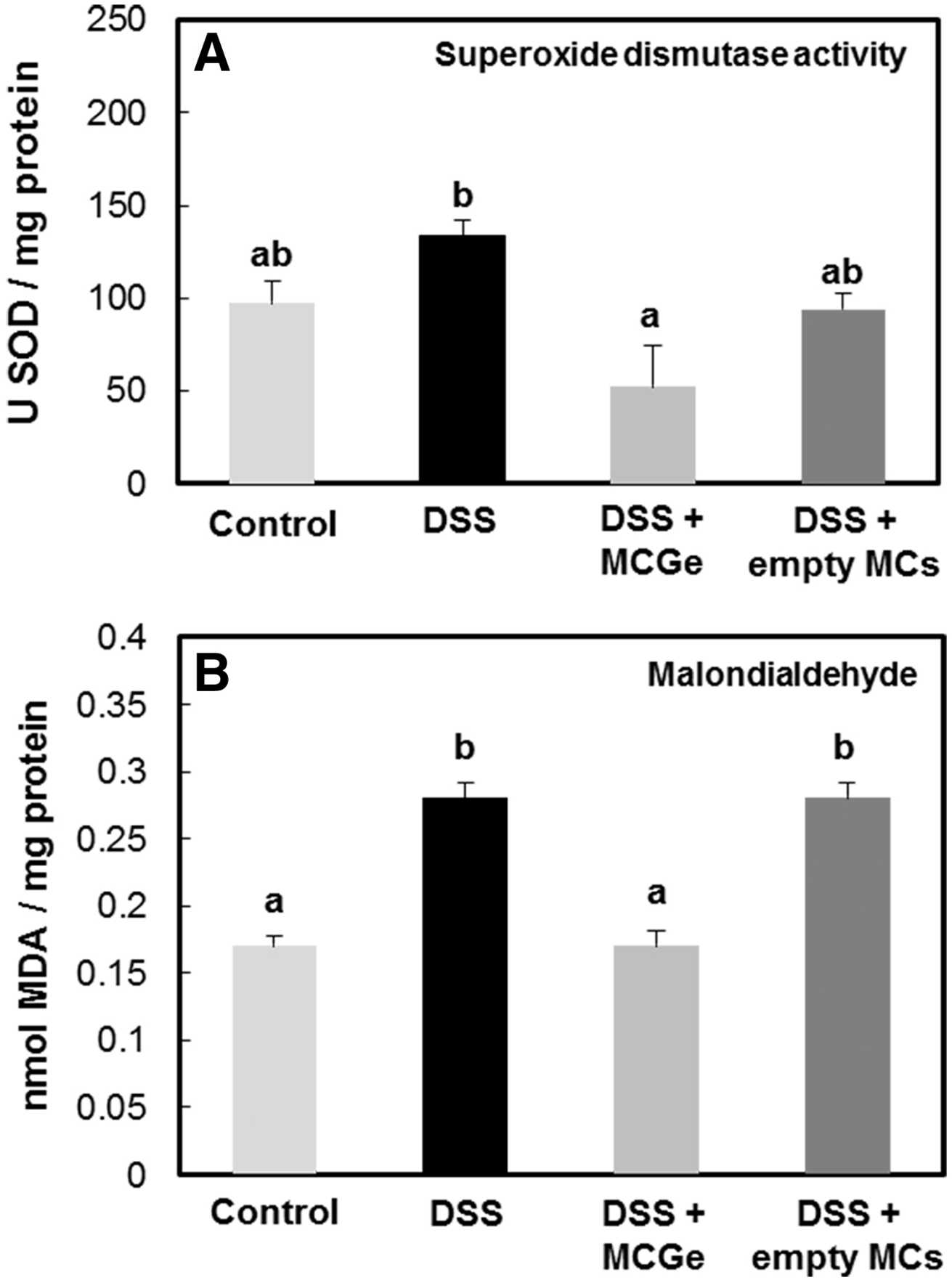
A
Superoxide dismutase activity
U SOD / mg protein
250
200
150
100
50
0
ab
b
a
ab
Control
DSS
DSS + MCGe
DSS + empty MCs
B
Malondialdehyde
nmol MDA / mg protein
0.4
0.35
0.3
0.25
0.2
0.15
0.1
0.05
0
a
b
a
b
Control
DSS
DSS + MCGe
DSS + empty MCs

Figure 6

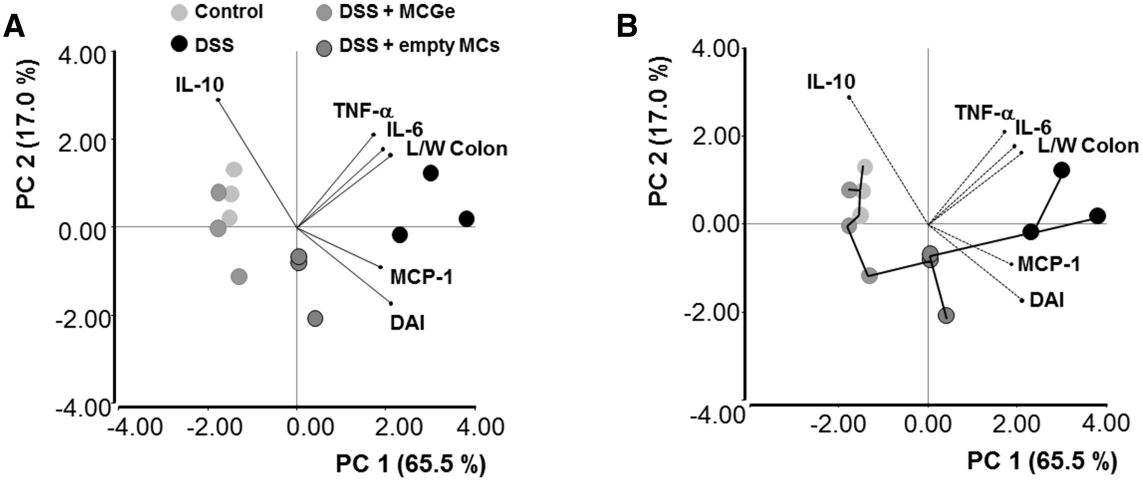

C

	DAI	L/W colon	TNF-α	IL-6	MCP-1	IL-10	SOD	MDA	MPO
DAI	*1*								
L/W colon	*0.64*	*1*							
TNF-α	*0.57*	*0.73*	*1*						
IL-6	*0.55*	*0.78*	*0.64*	*1*					
MCP-1	*0.64*	*0.71*	*0.23*	*0.62*	*1*				
IL-10	***-0.90***	***-0.39***	***-0.39***	***-0.30***	***-0.55***	***1***			
SOD	*0.53*	*0.81*	*0.64*	*0.48*	*0.50*	*-0.30*	*1*		
MDA	*0.75*	*0.53*	*0.36*	*0.43*	*0.52*	*-0.50*	*0.50*	*1*	
MPO	*0.89*	*0.74*	*0.68*	*0.45*	*0.51*	*-0.78*	*0.66*	*0.59*	*1*

Figure 7

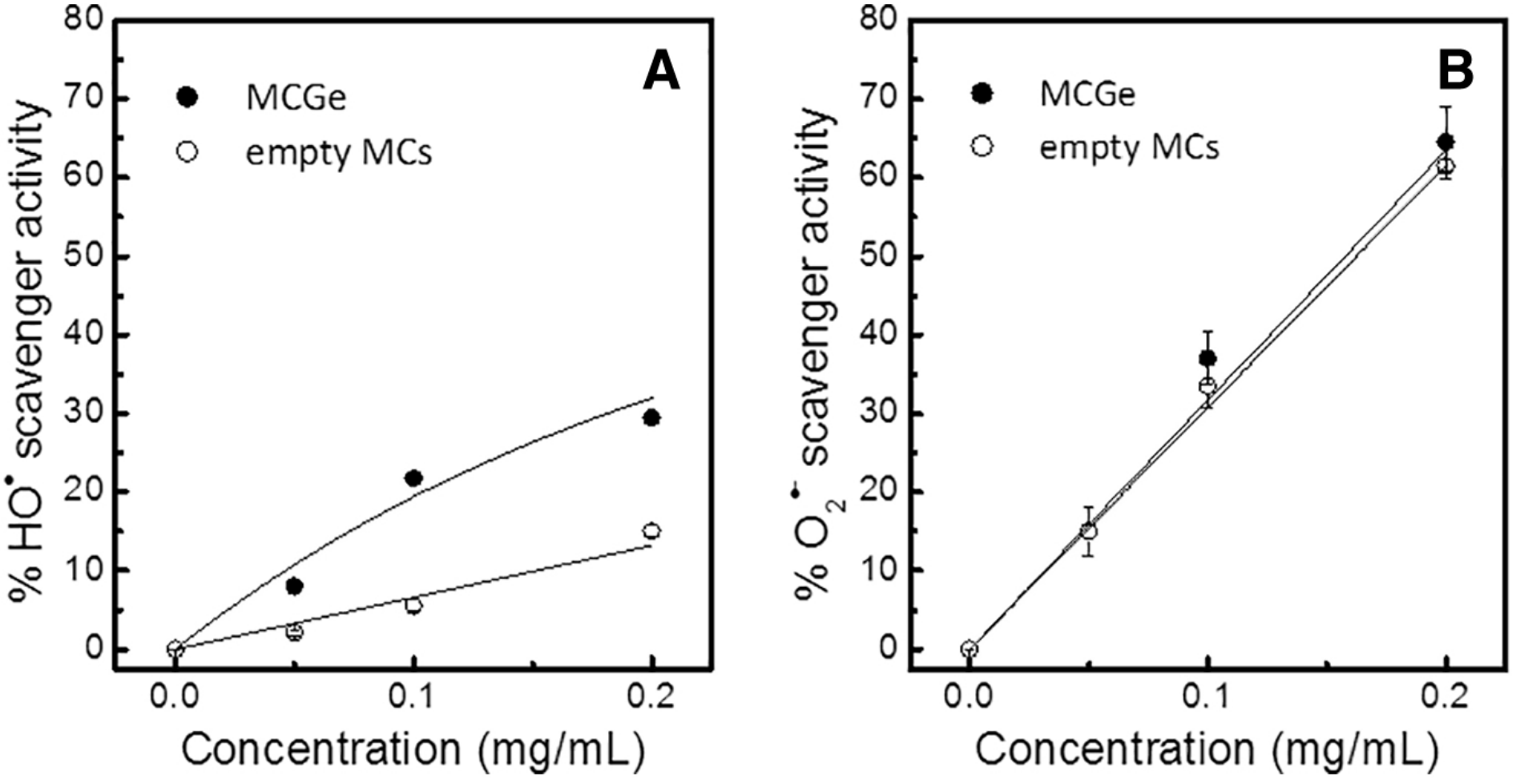
A
MCGe
empty MCs
% HO• scavenger activity
Concentration (mg/mL)
0
10
20
30
40
50
60
70
80
0.0
0.1
0.2
B
MCGe
empty MCs
% O2•- scavenger activity
Concentration (mg/mL)

Figure 8

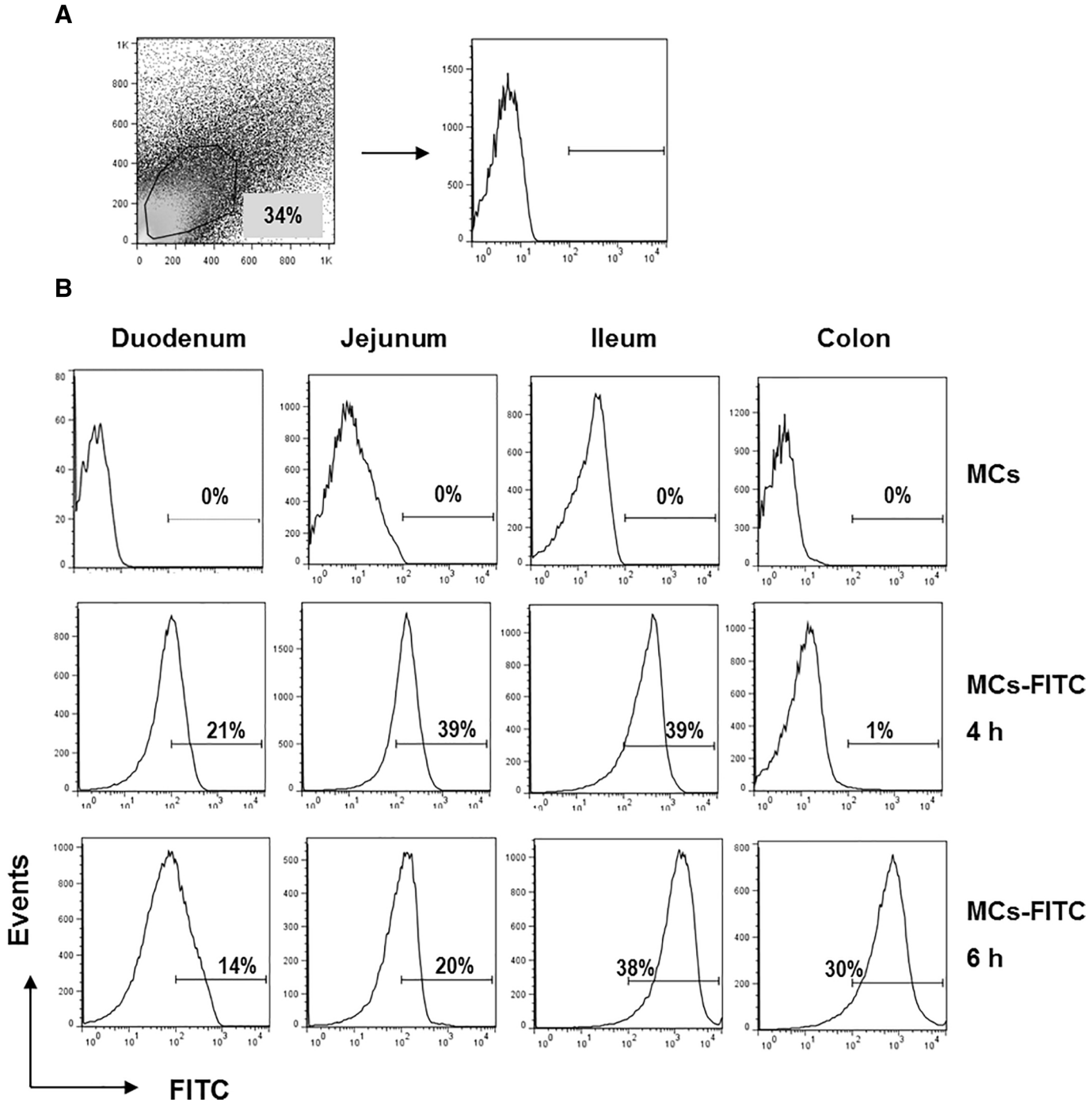
A
34%
B
Duodenum
Jejunum
Ileum
Colon
MCs
MCs-FITC
4 h
MCs-FITC
6 h
0%
21%
39%
39%
1%
14%
20%
38%
30%
Events
FITC

Figure 9

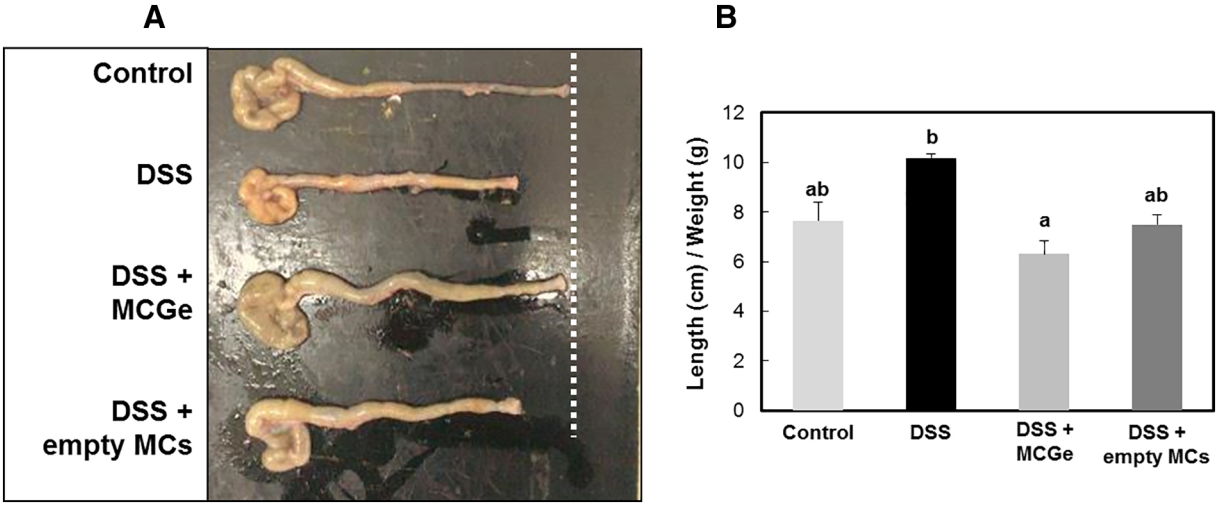
A
Control
DSS
DSS +
MCGe
DSS +
empty MCs
B
Length (cm) / Weight (g)
0
2
4
6
8
10
12
ab
b
a
ab
Control
DSS
DSS +
MCGe
DSS +
empty MCs

Figure 10

A. Disease Activity Index (DAI) in mice treated with pure Ge.

Group	DAI on day 10
Control	0.5 ± 0^{a}
DSS	7.67 ± 1.33^{b}
DSS + Ge	8 ± 1^{b}

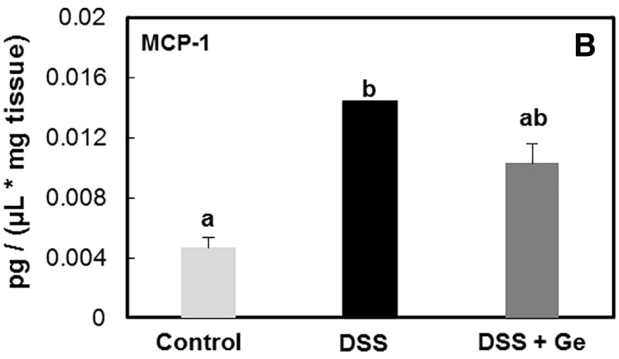

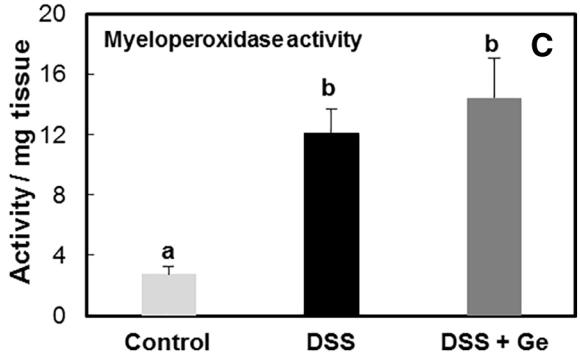

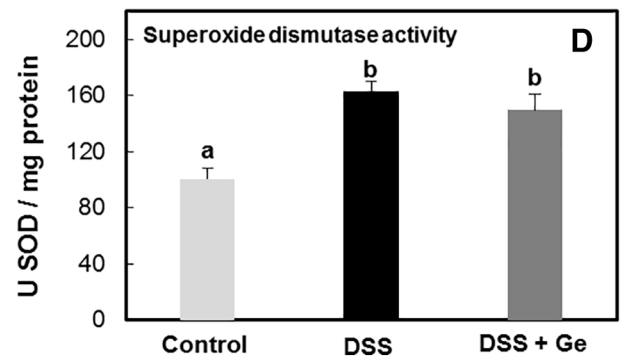

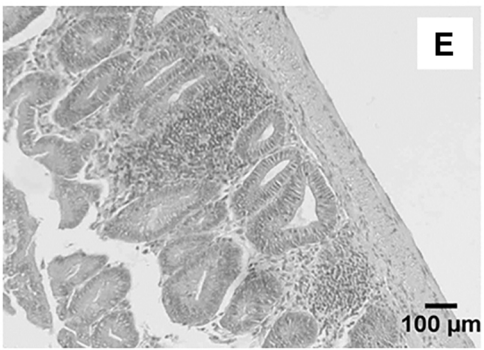

Figure 11